Chemical Engineering Journal 166 (2011) 624–630

Contents lists available at ScienceDirect

Chemical Engineering Journal

journal homepage: www.elsevier.com/locate/cej

Binding mechanisms and QSAR modeling of aromatic pollutant biosorption on *Penicillium oxalicum* biomass

Yu Zhang[a], Dongbin Wei[a], Rongde Huang[a], Min Yang[a,*], Shujun Zhang[b], Xiaomin Dou[a], Dongsheng Wang[a], Vipasiri Vimonses[c]

[a] State Key Laboratory of Environmental Aquatic Chemistry, Research Center for Eco-Environmental Sciences, Chinese Academy of Sciences, P.O. Box 2871, Beijing 100085, China
[b] The Administrative Center for China's Agenda 21, Ministry of Science and Technology, Beijing 100038, China
[c] Australian Water Quality Centre, SA Water Corporation, 250 Victoria Square, Adelaide,, SA 5100, Australia

ARTICLE INFO

Article history:
Received 1 September 2010
Received in revised form 8 November 2010
Accepted 8 November 2010

Keywords:
Biosorption
Penicillium oxalicum
Aromatic compounds
QSAR
PSA

ABSTRACT

The biosorption of eight aromatic compounds with different functional groups by *Penicillium oxalicum* biomass were investigated. The affinity of the biomass for the eight compounds at pH 6.0 follows the following trend: 1-naphthalenamine > naphthol > benzoic acid > *p*-toluidine > *p*-cresol > *p*-toluic acid > phenol > *p*-toluenesulfonic acid. Biomass surface was characterized, and it was found that four discrete binding sites, corresponding to carboxyl ($pK_a = 4.0$), phosphoric ($pK_a = 7.0$), amine ($pK_a = 8.8$), and hydroxyl groups ($pK_a = 10.0$), were identified on the biomass surface by using the linear programming method (LPM) for the fitting of the titration data and FTIR analysis. The carboxyl and amine groups dominate the biomass surface sites, which might have played an important role in biosorption of organic compounds. Furthermore, the compounds were divided into two groups based on the calculation of ionization degree for toluene derivatives and the comparison on the number of benzene rings for barely ionized compounds. It was found that low ionization degree and high hydrophobicity favor the biosorption for the two groups, respectively. Moreover, a R^2_{adj} of 0.724 between the log of Freundlich coefficient ($\log K_f$) and log *K*ow indicated that the hydrophobicity plays role in the sorption of eight organic compounds. The QSAR model with one variable was developed for the first time between $\log K_f$ and polar surface area (PSA) to predict the biosorption behaviors of organic compounds ($R^2_{adj} = 0.960$) except for *p*-toluenesulfonic acid (with $pK_a < 0$), which also supported the electrostatic attraction and hydrophobicity mechanisms.

1. Introduction

In modern society, an increasing number of hazardous compounds are being discharged into the water environment. The use of living or non-living biomass such as algae, bacteria, and fungi for the sorption of water pollutants has been widely focused due to their low cost, tolerance to toxicity, and the possibility for resource recovery [1–4]. Removal and recovery of heavy metals by biosorption has been extensively studied, and it is now clear that biosorption of heavy metals can be attributed to ion exchange, electrostatic interaction and covalent bonding of metal ions with the biosorption sites, or a combination of all three [5,6].

In comparison with biosorption of heavy metals, which can be characterized by some surface spectroscopic techniques such as electron dispersive spectroscopy (EDS) and X-ray photoelectron spectroscopy (XPS) [6–8] study on biosorption of organic pollutants have been difficult because traditional surface analysis techniques are ineffective in identifying the precise adsorption sites and characterizing structural changes caused by biosorption as both the adsorbents and adsorbates are organic [7,9,10]. So the acid–base titration technique has been used to probe the nature of surface sites on microbial biomass [11], the results of which could be used to produce a pK_a spectrum to determine the minimum number of components (sites) necessary to describe the data as well as the site concentrations by using some models like the linear programming method (LPM) [12–14].

On the other hand, biosorption of organic pollutants is far more complicated than that of heavy metals because the organic compounds possess a wide range of structural and molecular weight distributions [7,9,10]. Biosorption of organic pollutants can be affected by the organic adsorbate properties, such as molecular size, charge, solubility, and hydrophobicity. Three anionic reactive dyes with different reactive groups were used as models to investigate binding mechanisms by comparing their respective biosorption pattern on *Corynebacterium glutamicum* [15]. Electrostatic interaction and chemical bonding between the biomass surface and

* Corresponding author. Tel.: +86 10 62923475; fax: +86 10 62923541.
E-mail address: yangmin@rcees.ac.cn (M. Yang).

1385-8947/$ – see front matter © 2010 Elsevier B.V. All rights reserved.
doi:10.1016/j.cej.2010.11.034

Table 1
The structure, log *K*ow, pK_a, and calculated ionization rates of chemicals used as adsorbates.

Compound no.	Chemical	CAS no.	Structure	log *K*ow [49]	pK_a [37]	Ionized degree% (pH = 6.0)
Compd 1	Phenol	108-95-2	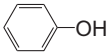	1.46	9.99	0.0
Compd 2	*p*-Cresol	106-44-5	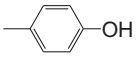	1.94	10.26	0.0
Compd 3	Naphthol	1321-67-1		2.85	9.30	0.1
Compd 4	*p*-Toluidine	106-49-0	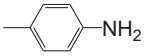	1.39	5.08	10.7
Compd 5	1-Naphthalenamine	134-32-7		2.25	3.92	0.8
Compd 6	Benzoic acid	117500-35-3	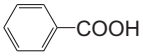	1.87	4.20	98.4
Compd 7	*p*-Toluic acid	99-94-5	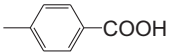	2.27	4.37	97.7
Compd 8	*p*-Toluenesulfonic acid	104-15-4	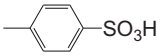	0.99	−1.34	100.0

dye reactive groups were speculated to be responsible for biosorption under acidic and basic pH conditions, respectively. It has been hypothesized that solubility and pK_a of phenols are two major factors affecting biosorption of phenol, mono, di- and trichlorophenols, and mono-nitrophenols on activated sludge [16]. However, due to the existence of diverse organic pollutants with different structures, more studies are required to establish the relationship between the chemical structure of organic pollutants and microbial sorption [9]. The quantitative structure–activity relationship (QSAR) technique has been considered to be useful to predict the adsorption behaviors of organic compounds on different adsorbents based on their chemical structures [17,18]. To our knowledge, however, few studies have been conducted on the interaction of organic compounds and microbial biomass.

In the present study, a filamentous fungal isolate (*Penicillium oxalicum*) showing high adsorption capacities for an anthraquinone-based dye (reactive blue 19) and two azo dyes (reactive red 241 and reactive yellow 145 (Fig. S1) [19] was used as a model biomass for the study of biosorption mechanism of organic compounds. The objectives of this study were (i) to characterize the surface properties of sterilized *P. oxalicum* biomass by combining FTIR analysis with acid–base titration fitted by the LPM; (ii) to investigate the relationship between the chemical structure of organic pollutants and microbial sorption by comparing their respective biosorption patterns and QSAR technique for eight aromatic compounds with functional groups. This study will enhance the understanding of biosorption mechanisms of organic pollutants.

2. Materials and methods

2.1. Biomass preparation and chemicals

The strain *P. oxalicum* (CGMCC No. 0810), stored in the China General Microbiological Culture Collection Center, was previously isolated from dye-contaminated soil samples [19]. It was grown in a liquid medium containing (g/L) glucose 10.0; KH_2PO_4 1.0; $(NH_4)_2SO_4$ 1.0; $MgSO_4{\cdot}7H_2O$, 0.5; pH 5.2. The culture was inoculated and cultivated at 30 °C in a shaker incubator at 150 rpm for 48 h. Mycelium pellets were separated from the growth medium by filtration and washed with de-ionized water. The biomass was sterilized for 15 min at 121 °C and 124 kPa to kill the fungus, preventing bioaccumulation and biodegradation of the chemicals in the subsequent adsorption experiments. The biomass was then rewashed with de-ionized water before centrifuged at 500 rpm for 10 min to remove the excess water. Biomass of a given wet weight was then used as adsorbent in the biosorption experiments.

Eight aromatic derivatives, i.e. phenol, *p*-cresol, naphthol, *p*-toluidine, 1-naphthalenamine, benzoic acid, *p*-toluic acid, and *p*-toluenesulfonic acid, were used as surrogate compounds in this study. The molecular structures and some physico-chemical characteristics of these derivatives are given in Table 1 and Table S1. All chemicals were of analytical grade, purchased from the Beijing Chemical Industry.

2.2. Adsorption experiment

Biosorption experiments were conducted in batch adsorption equilibrium experiments. Approximately 25 ml of aqueous solutions of target compounds with different concentrations (in the range of 10–100 mg/l) were mixed with 0.25 g biomass (wet weight with approximately 85% water content) at a pH of 6.0 in Erlenmeyer flasks sealed with PARAFILM^{TM}. The suspension was shaken at 30 °C in a rotary shaker at 150 rpm for 24 h, before the residual aqueous concentration of each compound was measured using a Waters Series HPLC system (Model 515 pump and 2996 photodiode array detector, Waters Assoc., Milford, MA, USA) equipped with an Agilent C18 reversed-phase column (20RBAX SB-C18). The mobile phase consisted of methanol and 0.02 M ammonium acetate buffer at a flow rate of 1.0 ml/min. These compounds were detected at their maximum adsorption wavelength by the 2996 PDA detector. The biomass was weighed after drying at 80 °C for 24 h. All experiments were performed in duplicate. The adsorption capacity at equilibrium, *Q* (mmol/g), was calculated using Eq. S1. The Freundlich and Langmuir isotherm equations (Eqs. S2 and S3) were used to describe the biosorption equilibrium data.

2.3. Surface characteristics of P. oxalicum biomass

The electrophoretic mobility of the biomass was measured using a Zetasizer 2000, Malvern Instruments. The FTIR spectra of biomass (dried at 60 °C) were recorded on a Nicolot MexuS system 670 spectrophotometer. All acid–base titrations were carried out in a constant-temperature/pressure variable volume airtight reactor using an automatic acid–base titration (665-Dosimat682; Merohm; Swiss). The titration data were analyzed using LPM of Discrete Sites Analysis (DISI) to characterize the functional groups of the biomass surface based upon the method suggested in the previous studies [11,14,20,21]. Detailed information on biomass surface characteristics and LPM data analysis for pK_a spectra are shown in Supporting Information together with the potentiometric titration results.

2.4. Molecular descriptors for QSAR

Twenty-eight molecular structure descriptors and one physicochemical parameter (log *K*ow) of the test chemicals were calculated based on PM3 method using Chemoffice software (Ver. 2005) and Estimation Programs Interface SuiteTM software [22], respectively. Major structural descriptors include, heat of formation (HOF), electronic energy (EE), total energy (TE), and Gibbs energy (GE) mainly reflecting the thermodynamic information of the chemical molecules; the maximum positive charge of H atom (qH^+) and the maximum negative charge of atom (Q^-) showing the electrostatic characteristics of the chemical molecules; the highest occupied molecular orbital energy (E_{homo}) and the lowest unoccupied molecular orbital energy (E_{lumo}) describing the molecular orbital information; ionization potential (IP), polar surface area (PSA), and dipole moment (DM) reflecting the polarity/dipole properties of the chemicals; and the molecular connectivity indices, e.g. Wiener index (WI), total valence connectivity index (TVCI), molecular topological index (MTI), and Randic connectivity index (RCI) were used to reflect information on shape, size, and area of the objective chemicals [23–26].

3. Results

3.1. Surface characteristics of P. oxalicum biomass

Fig. S2 shows the zeta potential values of *P. oxalicum* biomass as a function of pH, which reveals that the isoelectric point value was approximately pH 5.5. For characterizing heterogeneous biomass surface binding sites, an LPM fitting of the potentiometric titration (ionic strength = 0.1 mol/L) results for the biomass surface (Fig. S3) and the pK_a spectrum of the four main binding groups were obtained as shown Fig. 1. The corresponding estimation of binding site concentrations and pK_a values are listed in Table 2. There are clusters of ligand sites with pK_a values at 4.0 (0.43 mmol/g), 7.0 (0.20 mmol/g), 8.8 (0.37 mmol/g), and 10.0 (0.62 mmol/g). The first site (pK_a, 4.0) was assigned to carboxylic groups in biological polymers [11,20,21,27], which are very close to the fungal cell wall [28]. The second site (pK_a, 7.0), which showed the lowest concentration, was assigned to phosphoric groups of phospholipids [11,21]. The last two sites (pK_a, 8.8 and 10.0) were assigned to amine and hydroxyl groups, respectively [21,28,29].

In order to confirm the existence of above ligand sites on the *P. oxalicum* biomass surface, an FTIR analysis was carried out, as shown in Fig. 2. In the region of 2000–1500 cm^{-1}, the spectra were dominated by the vibration of the peptide backbone [30]. The band at 1747 cm^{-1} was identified as the C=O vibration of carboxylic groups, which is derived primarily from the ester linkage of fatty aliphatic monocarboxylic acids [31,32]. Amide bands were found at 1642 cm^{-1} (amide I band), 1537 cm^{-1} (amide II band), and 1454 cm^{-1} (amide III band) [30,33]. Symmetric and asymmetric stretching vibrations of P=O in nucleic acids were identified at 1040 and 1232 cm^{-1} [31]. The band near 3300 cm^{-1} showed the surface hydroxyl groups [30,34].

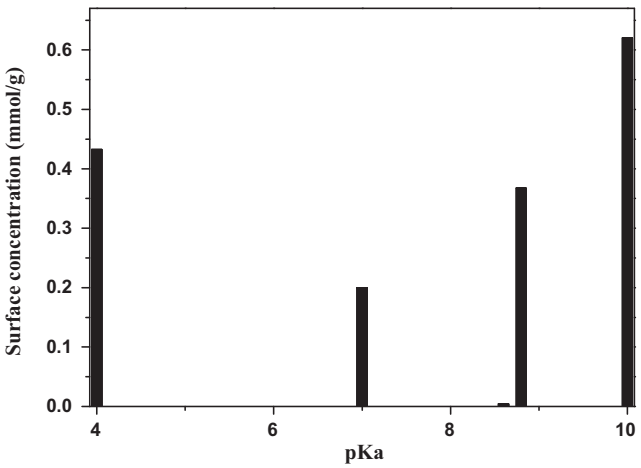

Fig. 1. pK_a spectra for *P. oxalicum* biomass surface (ionic strength = 0.1 mol/L).

Table 2
Values and site densities for four proposed sites on biomass surface.

Site no.	pK_a	Concentration (mmol/g of dry biomass)	Proposed surface site
1	4.0	0.43	Carboxylic
2	7.0	0.20	Phosphoric
3	8.8	0.37	Amines
4	10.0	0.62	Hydroxyl

3.2. Biosorption equilibrium isotherms of different aromatic compounds

The Langmuir and Freundlich equations were used to fit the adsorption isotherms of the eight organic compounds at a given concentration range and pH of 6.0. The Langmuir (assuming monolayer coverage of the adsorbate on the homogenous surface of the adsorbent) and Freundlich (assuming heterogeneous surface of the adsorbent) equations were used to fit the adsorption isotherms of the eight organic compounds at a given concentration range and pH of 6.0. As shown in Table 3, the Freundlich equation showed a better fit ($R^2 > 0.8$) for all eight compounds,

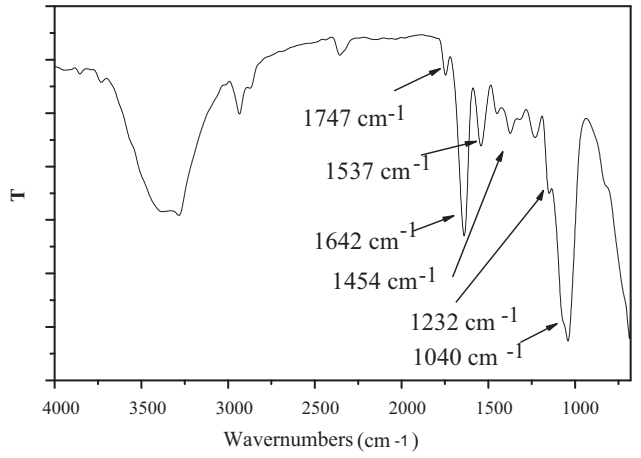

Fig. 2. FTIR spectra of *P. oxalicum* biomass surface.

Table 3
Comparison of constants of Langmuir and Freundlich equations.

Chemical	Langmuir equation			Freundlich equation		
	Q_m (mmol/g)	K (L/mmol)	R^2	K_f	n	R^2
Phenol	0.011	1.10	0.998	0.012	8.66	0.916
p-Cresol	0.022	0.02	0.941	0.018	1.74	0.925
Naphthol	0.058	0.02	0.960	0.056	1.60	0.968
p-Toluidine	0.032	0.01	0.994	0.020	1.47	0.994
1-Naphthalenamine	0.150	0.01	0.977	0.078	1.24	0.994
Benzoic acid	–	–	–	0.025	0.81	0.926
p-Toluic acid	–	–	–	0.016	1.15	0.827
p-Toluenesulfonic acid	0.007	0.03	0.987	0.007	2.02	0.957

perhaps due to the fact that biomass adsorbents generally possess multiple functional groups on their surfaces [5,27,35]. The Freundlich coefficient (K_f: the indicators of the "adsorption capacity") of the eight compounds at pH 6.0 decreased in the following order: 1-naphthalenamine (K_f = 0.078) > naphthol (0.056) > benzoic acid (0.025) > *p*-toluidine (0.020) > *p*-cresol (0.018) > *p*-toluic acid (0.016) > phenol (0.012) > *p*-toluenesulfonic acid (0.007).

3.3. Calculation of the adsorbate ionization degrees

Ionization degree, which is related to the electrostatic properties of organic compounds, was calculated by the ratio of dissociated ion ($[A^-]$) to the total concentration ($[A^-] + [HA]$) [36], according to Eqs. (1) and (2):

$$\mathrm{pH} = \mathrm{p}K_a + \log\frac{[A^-]}{[HA]} \quad (1)$$

$$\mathrm{Ionized\%} = \frac{100}{1 + 10^{(\mathrm{charge}(\mathrm{pH}-\mathrm{p}K_a))}} \quad (2)$$

where charge = 1 for bases and −1 for acids. The pK_a values [37] and the ionization degree for different compounds at pH 6.0 are listed in Table 1. The ionization degrees at pH 6.0 varied extremely from 0 to 100%, indicating the different electrostatic properties of organic compounds.

3.4. Quantitative estimation of biosorption by QSAR models

The $\log K_f$ of eight compounds were correlated with 29 corresponding molecular structure descriptors (Table S2). All of them, however, showed very poor fitting except for log *K*ow (log of the octanol/water partition coefficient). The correlation between log *K*ow and $\log K_f$ is shown in Eq. (3):

$$\log K_f = 0.511 \log K\mathrm{ow} - 2.578 \quad (3)$$

$$n = 8,\ R^2 = 0.764,\ R^2_{\mathrm{adj}} = 0.724,\ \mathrm{SD} = 0.181,$$

$$F = 19.373,\ p < 0.005$$

where n is the number of samples in the training set, R^2 is the multiple correlation coefficient, R^2_{adj} is the adjusted multiple correlation coefficient, SD is the standard deviation, F is the value of the F-test, and p is the significance level. A robustness test for Eq. (3) was performed by using the leave-one-out cross-validation [38,39], and the test results are shown as a radar plot in Fig. S5. It is considered that the robustness of a model is determined by the stability of R^2_{adj} when the corresponding compound is deleted in the leave-one-out method. Deterioration of R^2_{adj} stability was observed when compound 8 (*p*-toluenesulfonic acid) was deleted, as shown in Fig. S5. So compound 8 is a special compound which may affect the quality of this model.

So, the relationships between the $\log K_f$ for the remaining 7 compounds and the 29 molecular connectivity indices were respectively explored, and the statistical results are summarized in Table S3. Among them, seven variables, i.e. MT1, ^{1}X, TVCI, WI, PSA, MR, and CSEV showed good fitting to $\log K_f$ ($R^2_{\mathrm{adj}} = 0.902 - 0.975$) and became statistically significant, as shown in Eqs. (4)–(8).

$$\log K_f = 0.001\,\mathrm{MTI} - 2.218 \quad (4)$$

$$n = 7,\ R^2 = 0.979,\ R^2_{\mathrm{adj}} = 0.975,\ \mathrm{SD} = 0.046,$$

$$F = 231.86,\ p < 0.001$$

$$\log K_f = 0.363\,{}^1\mathrm{X} - 3.133 \quad (5)$$

$$n = 7,\ R^2 = 0.967,\ R^2_{\mathrm{adj}} = 0.961,\ \mathrm{SD} = 0.058,$$

$$F = 147.88,\ p < 0.001$$

$$\log K_f = 1.465\,\mathrm{WI} - 5.712 \quad (6)$$

$$n = 7,\ R^2 = 0.959,\ R^2_{\mathrm{adj}} = 0.951,\ \mathrm{SD} = 0.064,$$

$$F = 117.34,\ p < 0.001$$

$$\log K_f = 0.007\,\mathrm{TVCI} - 2.200 \quad (7)$$

$$n = 7,\ R^2 = 0.950,\ R^2_{\mathrm{adj}} = 0.939,\ \mathrm{SD} = 0.071,$$

$$F = 94.13,\ p < 0.001$$

$$\log K_f = -8.577\,\mathrm{PAS} - 1.0141 \quad (8)$$

$$n = 7,\ R^2 = 0.967,\ R^2_{\mathrm{adj}} = 0.960,\ \mathrm{SD} = 0.05791,$$

$$F = 145.83,\ p < 0.001$$

$$\log K_f = 0.041\,\mathrm{MR} = 3.065 \quad (9)$$

$$n = 7,\ R^2 = 0.938,\ R^2_{\mathrm{adj}} = 0.926,\ \mathrm{SD} = 0.07896,$$

$$F = 76.130,\ p < 0.001$$

$$\log K_f = 0.019\,\mathrm{CSEV} - 3.448 \quad (10)$$

$$n = 7,\ R^2 = 0.919,\ R^2_{\mathrm{adj}} = 0.902,\ \mathrm{SD} = 0.09077,$$

$$F = 56.391,\ p < 0.001$$

To determine the robustness of developed PSA model, the leave-one-out method was also used for Eq. (8) and the results show that all of R^2_{adj} values of compound 1–7 in radar plot (Fig. 3(c)) were similar, and the frequency distribution of residuals obeys normal function (Fig. 3(b)). On the other hand, the correlation coefficient (q^2) and root mean squared error of validation (RMSEV), which is also employed to evaluate the QSAR model internal prediction error, were calculated as 0.925 and 0.087, respectively. This indicates that the developed QSAR equation (8) had good robustness, and could be used to estimate the biosorption behavior of studied compounds effectively (Fig. 3(a)).

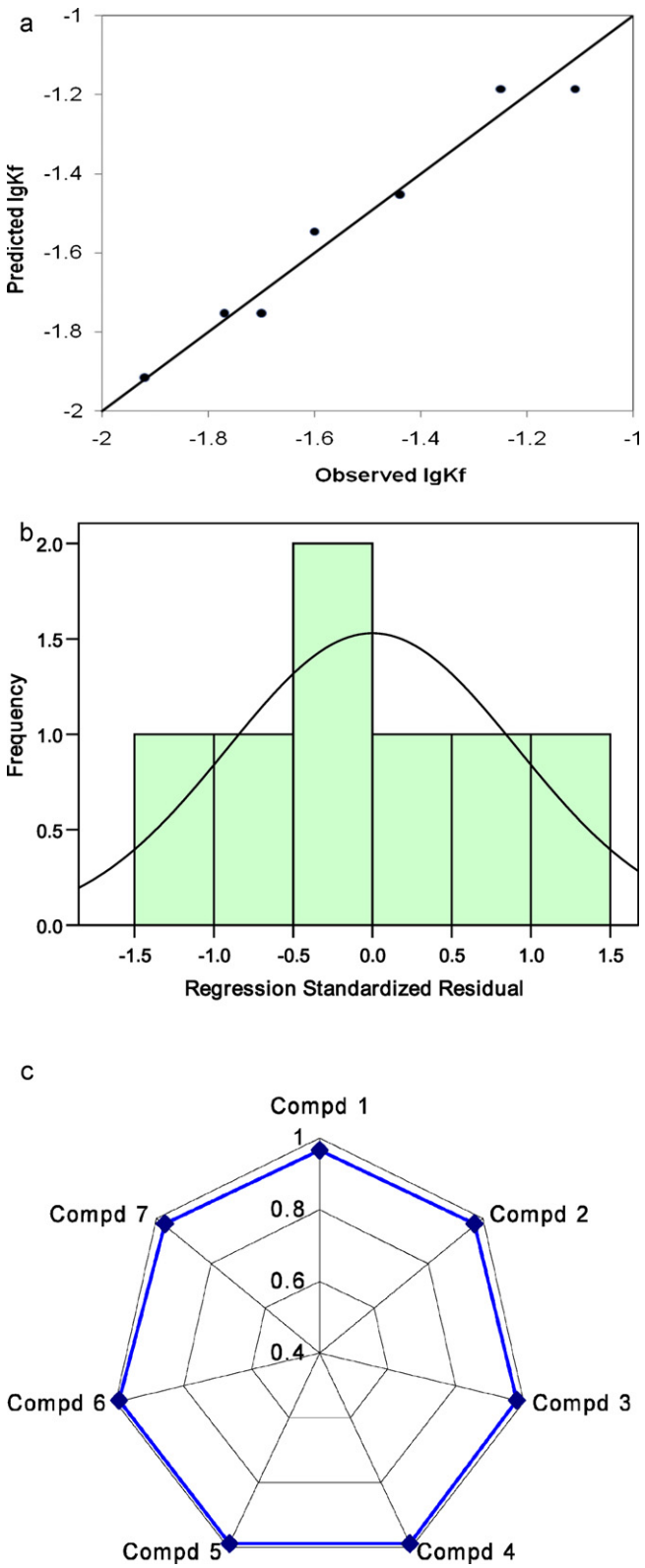

Fig. 3. (a) The plot of observed $\log K_f$ vs. predicted $\log K_f$ from Eq. (8); (b) the frequency distribution of residuals for Eq. (8); (c) the distribution of correlation coefficients with leave-one-out test in Eq. (8) (the value on the axis reflects the R^2_{adj} when the corresponding compound has been deleted).

4. Discussion

Biosorption of the hazardous organics from wastewater by selected live and dead microorganisms has been investigated by various workers; however, the lack of understanding of the biosorption mechanism hinders the satisfactory estimation of process performance, and thus the widespread application of the technology.

One of the major difficulties for studying biosorption mechanisms of organic pollutants was that traditional surface analysis techniques are ineffective in identifying the precise adsorption sites and characterizing structural changes caused by biosorption. So we employed the LPM to fit the titration data for characterizing heterogeneous biomass surface binding sites. Our results indicate that there are four discrete binding sites, carboxyl ($pK_a = 4.0$), phosphoric ($pK_a = 7.0$), amine ($pK_a = 8.8$), and hydroxyl ($pK_a = 10.0$), on the biomass surface (Fig. 1 and Table 2), which was supported by the FTIR data (Fig. 2).

The total site concentration (dry weight: 1.62 mmol/g; wet weight: 0.24 mmol/g obtained by recalculating to concentration of wet weight of biomass by considering the water content (about 85%) of the biomass before drying) of *P. oxalicum* biomass at 0.1 mol/L ionic strength (IS) was in accordance with those of *Saccharomyces cerevisiae* (wet weight: 0.17 mmol/g) [40], Gram-positive bacteria *B. subtilis* (wet weight: 0.32 mmol/g) [29], and most Gram-negative bacteria reported (dry weight: 0.078–1.66 mmol/g) [31] at the same IS. Although the total site densities are of the same order of magnitude, the distribution of binding groups appeared to be quite different. Gram-positive bacteria possess higher phosphoric groups (dry weight: 0.44–0.83 mmol/g) than the Gram-negative bacteria (dry weight: 0.19–0.44 mmol/g) [31] and that in our study (dry weight: 0.20 mmol/g), perhaps because its cell envelope is surrounded by a thick external layer of petidoglycan [29]. In the present study, it is clear that the carboxyl, amine, and hydroxyl groups existed at a relatively high site concentration on the fungus cell surface, which might be attributed to chitin, acidic polysaccharides, lipids, amino acids, and other components on the surface [31].

As previously reported, low pH favors biosorption of three reactive dyes by *P. oxalicum* biomass [19]. The isoelectric point value of pH 5.5 should be the comprehensive interaction results of different surface binding groups. Weaker base groups on the biomass surface become positively charged at pH < 5.5 [41], which was favorable for the adsorption of negatively charged reactive dyes in aqueous solution. Most of the amine groups are protonated at a pH below 8.8, playing an important role in the electrostatic attraction toward the negatively charged sites of organic compounds. A similar result has been reported by Won et al. [21], on the adsorption of negatively charged reactive day by *D. glutamicum*. The carboxyl group which has been proved to be the main origin for metal binding [42], on the other hand, might also play an important role in the electrostatic attraction toward the positively charged sites of organic compounds. At the same time, the repulsion effects of the carboxyl groups toward the strong acid groups such as sulfonic acid of organic compounds could lead to the decrease of biosorption capacity at high pH. The studies on the role of hydroxyl groups, which have been reported to play an important role in the biosorption of heavy metals [42], have been scarce.

Another major challenge of study on biosorption mechanism of organic pollutants was that the organic compounds possess a wide range of structural and molecular weight distributions. To understand the relationship between the chemical structure of organic pollutants and microbial sorption, eight aromatic compounds with different benzene numbers and/or functional groups were used as model chemicals on the biosorption of *P. oxalicum*. Both Fig. S4(a) and Table 3 show that the adsorption capacity of

toluene derivatives at pH 6.0 decreased in the following order: *p*-toluidine > *p*-cresol > *p*-toluic acid > *p*-toluenesulfonic acid. At pH 6.0, the weakly acidic carboxyl groups on the biomass surface were mostly ionized (such as R-COO^-), contributing to the biomass's overall negative surface charge. At the same time, the ionization states of the adsorbates were also affected by solution pH. According to calculation of the ionization degree of four toluene derivatives at pH 6.0 (Table 1), *p*-toluic acid and *p*-toluene sulfonic acid were both deprotonated and negatively charged. *p*-Cresol, a weak acid with a pK_a value higher than the solution pH, was present in its non-dissociated form. *p*-Toluidine, a weak base with a pK_a value similar with the solution pH, was only slightly ionized in the solution. For *p*-toluidine and *p*-cresol, the amine group (–NH_2) and hydroxyl group (–OH) attached to the aromatic rings were electron donating groups, which push the electron cloud toward the benzene rings to transform into partially positively charged surface [43]. Consequently, the higher K_f of *p*-cresol and *p*-toluidine (Fig. S4(a)) may be due to electrostatic attraction between negatively charged cell surface sites (such as R-COO^-,) and partially positively charged functional groups of these aromatic compounds.

To further investigate the effect of pH on biosorption, the isotherms of *p*-toluenesulfonic acid at pH 3.0 and 6.0 were compared (Fig. S4(b)). The values of K_f were calculated to be 0.16 and 0.007 at pH 3.0 and pH 6.0, respectively. The increased adsorption of *p*-toluenesulfonic acid under a lower pH was attributed to the electrostatic attraction between the negatively charged *p*-toluenesulfonic acid and the partially positively charged (R-NH_3^+) sites on the biomass surface [28].

On the other hand, *p*-cresol (K_f = 0.018), naphthol (K_f = 0.056), *p*-toluidine (K_f = 0.020) and 1-naphthalenamine (K_f = 0.078) were barely ionized at a pH ≈6.0 (Table 1). For this kind of group of compounds, the increase in the number of benzene rings from one to two corresponded well to the increase in biosorption capacities (Fig. S4(c)). As shown in Table 1, the log *K*ow increased with the increase in benzene rings from one to two, indicating the increase of adsorbate hydrophobicity might be one major reason for the increase in biosorption.

QSAR technique is considered as a useful tool for predicting relationships between the structure of organic molecules and microbial biosorption. Recently, correlating metal ionic characteristics with biosorption capacity of metal ions (n = 5–9) has been investigated by using QSAR models [44,45]. As described above, both ionization degree described by pK_a and pH, and hydrophobicity determined by log *K*ow were two important factors affecting biosorption performance of organic pollutants. It was found that pK_a could not be correlated with log K_f (data not shown). The R^2_{adj} (0.724) of Eq. (3) indicated that log *K*ow could be used to describe the sorption of organic compounds to biomass to some extent. Similar results have been reported on biosorption of chlorophenols to anaerobic granular sludge (R^2 < 0.6) [46].

On the other hand, some other factors might also affect biosorption behaviors. Therefore, we selected 29 commonly used molecular descriptors to develop QSAR models. All of them, however, showed very poor fitting (n = 8) (Table S2), which indicates special compound with different sorption mechanism might exist. The result of robustness test for Eq. (3) implies that *p*-toluenesulfonic acid was a special sample (Fig. S5).

When *p*-toluenesulfonic acid was deleted from training set, seven molecular connectivity indices can be used to estimate biosorption characteristics for the studied chemicals effectively (R^2_{adj} > 0.9) (Table S3). Among them, the molecular connectivity indices – MTI, ^{1}X, WI, TVCI, MR, and CSEV describes or reflects the size of chemical molecule, the bonds that connect the skeletal atoms, the size of molecule, a refinement of the molecular connectivity index, a measure of the total polarizability of a mole of a compound, and the volume contained within the contact molecular surface, respectively. All these parameters had a positive correlation with log K_f, which indicates that larger molecular size and molecular volume benefits biosorption. On the other hand, besides the good prediction ability (R^2_{adj}), the physicochemical meaning of parameter in equation and mechanism exploration should be paid more attention. PSA, a parameter combining shape and electronic information to characterize molecules, has clear physicochemical meaning [47]. It has been reported that PSA is related to the passive chemical molecule transport to target cell [48]. Significant negative correlation between log K_f and PSA of 7 compounds (Eq. (8)) indicates that less surface area of polar (or solvated) atoms favored biosorption. The similar R^2_{adj} values of the seven compounds (Fig. 3(c)) and good frequency distribution (Fig. 3(b)) indicate that the developed QSAR equation (8) had good robustness. Accordingly, the PSA model combining molecular shape and electronic information might be an appropriate model to estimate the biosorption behavior of studied compounds (except for *p*-toluenesulfonic acid) effectively (Fig. 3(a)). *P. oxalicum* biomass showed high adsorption capacities for an anthraquinone-based dye and two azo dyes (Fig. S1) [19]. So the selection of the eight model chemicals was mainly on the basis of structure information of the three kinds of dyes to investigate the biosorption mechanisms. It should be noted, however, more samples are required to establish a solid QSAR model for the prediction of biosorption.

p-Toluenesulfonic acid was a special sample in the training set of QSAR models, suggesting that a different interaction mechanism might be responsible for its biosorption. This compound contains a sulfonate group and shows an extremely low pK_a (−1.34), which might be responsible for its different biosorption behavior. So the biosorption mechanism for this type of compounds requires further studies.

5. Conclusion

The present study provides better understanding of the effects of molecular structure and biomass surface properties of the fungi toward different organic compounds. Four discrete binding sites were found to exist on the biomass surface, corresponding to carboxyl, phosphoric, amine, and hydroxyl groups. Based upon the characterization of biomass binding sites and compound properties, the electrostatic interaction and chemical hydrophobicity are two factors affecting the adsorption capacity. In quantitative study, the PSA model, for the first time, was developed for estimating adsorption behaviors of the studied chemicals except for *p*-toluenesulfonic acid (with pK_a < 0), which is in accordance with the electrostatic interaction and hydrophobicity mechanisms very well. Our results indicate the *P. oxalicum* biomass may represent an effective bisorbent for the removal of organic compounds from wastewater, and the quantitative results can be used to predict the biosorption ability of series of organic compounds of *P. oxalicum* biomass or similar fungal biomass as organic biosorbents. However, the biosorption mechanism of *p*-toluenesulfonic acid related compounds requires further studies.

Acknowledgment

This work was supported by the National Natural Science Foundation of China (No. 50921064) and the Special Co-construction Project of Beijing Municipal Commission of Education.

Appendix A. Supplementary data

Supplementary data associated with this article can be found, in the online version, at doi:10.1016/j.cej.2010.11.034.

References

[1] A. Kapoor, T. Viraraghavan, Fungal biosorption—an alternative treatment option for heavy metal bearing wastewaters: a review, Bioresour. Technol. 53 (1995) 195–206.
[2] T.A. Davis, A review of the biochemistry of heavy metal biosorption by brown algae, Water Res. 37 (2003) 4311–4330.
[3] K. Vijayaraghavan, Y.S. Yun, Bacterial biosorbent and biosorption, Biotechnol. Adv. 26 (2008) 266–291.
[4] K. Chojnacka, Biosorption and bioaccumulation—the prospects for practical applications, Environ. Int. 36 (2010) 299–307.
[5] W. Plazinski, W. Rudzinski, Modeling the effect of surface heterogeneity in equilibrium of heavy metal ion biosorption by using the ion exchange model, Environ. Sci. Technol. 43 (2009) 7465–7471.
[6] J.L. Wang, C. Chen, Biosorbents for heavy metals removal and their future, Biotechnol. Adv. 27 (2009) 195–226.
[7] B. Volesky, Biosorption and me, Water Res. 41 (2007) 4017–4029.
[8] J.R. Haas, Effects of cultivation conditions on acid–base titration properties of *Shewanella putrefacieds*, Chem. Geol. 209 (2004) 67–81.
[9] Z. Aksu, Application of biosorption for the removal of organic pollutants: a review, Process Biochem. 40 (2005) 997–1026.
[10] G. Crini, Non-conventional low-cost adsorbents for dye removal: a review, Bioresour. Technol. 97 (2006) 1061–1085.
[11] J.S. Cox, D.S. Smith, L.A. Warren, F.G. Ferris, Characterizing heterogeneous bacterial surface functional groups using discrete affinity spectra for proton binding, Environ. Sci. Technol. 33 (1999) 4514–4521.
[12] M. Borkovec, U. Rusch, J.C. Westall, in: E.A. Jenne (Ed.), Adsorption of Metals by Geomedia: Variables, Mechanisms and Model Applications., Academic Press, New York, 1998, Chapter 22.
[13] D. Smith, J. Kramer, Multi-site proton interactions with natural organic matter, Environ. Int. 25 (1999) 307–314.
[14] Y.S. Yun, B. Volesky, Modeling of lithium interference in cadmium biosorption, Environ. Sci. Technol. 37 (2003) 3601–3608.
[15] S.W. Won, M.H. Han, Y.S. Yun, Different binding mechanisms in biosorption of reactive dyes according to their reactivity, Water Res. 42 (2008) 4847–4855.
[16] N. Calace, E. Nardi, B.M. Petronio, M. Pietroletti, Adsorption of phenols by papermill sludges, Environ. Pollut. 118 (2002) 315–319.
[17] C. Brasquet, P.L. Cloirec, QSAR for organics adsorption onto activated carbon in water: what about the use of neural networks? Water Res. 33 (1999) 3603–3608.
[18] A. Sabljic, QSAR models for estimating properties of persistent organic pollutants required an evaluation of their environmental fate and risk, Chemosphere 43 (2001) 363–375.
[19] S.J. Zhang, M. Yang, Q.X. Yang, Y. Zhang, B.P. Xin, F. Pan, Biosorption of reactive dyes by the mycelium pellets of a new isolate of *Penicillium oxalicum*, Biotechnol. Lett. 25 (2003) 1479–1482.
[20] P. Brassard, J.R. Kramer, P.V. Collins, Binding site analysis using linear programming, Environ. Sci. Technol. 24 (1990) 195–201.
[21] S.W. Won, S.B. Choi, Y.S. Yun, Interaction between protonated waste biomass of *Corynebacterium glutamicum* and anionic dye Reactive Red 4, Colloids Surf. A 261 (2005) 175–180.
[22] http://www.epa.gov/opptintr/exposure/docs/episuite.htm.
[23] D.A. Bahnick, W.J. Doucette, Use of molecular connectivity indices to estimate soil adsorption coefficients for organic chemicals, Chemosphere 17 (1988) 1703–1715.
[24] L.B. Kier, L.H. Hall, Molecular Connectivity in Chemistry and Drug Research, Academic Press, New York/San Francisco/London, 1976.
[25] G. Schuurmann, Quantitative structure–property relationships for polarizability, solvatochromic parameters and lipophilicity, QSAR Comb. Sci. 9 (1990) 326–333.
[26] M. Martin, Quantum chemical modeling of soil sorption coefficients: multiple linear regression models, Chemosphere 35 (1997) 365–377.
[27] N. Saglam, R. Saya, D. Adil, S. Patır, M.Y. Arica, Biosorption of inorganic mercury and alkylmercury species on to *Phanerochaete chrysosporium* mycelium, Process Biochem. 34 (1999) 725–730.
[28] M.Y. Arıca, Ç. Arpa, A. Ergene, G. Bayramolu, O. Genç, Ca-alginate as a support for Pb(II) and Zn(II) biosorption with immobilized *Phanerochaete chrysosporium*, Carbohyd. Polym. 52 (2003) 167–174.
[29] J.B. Fein, C.J. Daughney, N. Yee, T.A. Davis, A chemical equilibrium model for metal adsorption onto bacterial surfaces, Geochim. Cosmochim. Acta 61 (1997) 3319–3328.
[30] L.G. Benning, V.R. Phoenix, N. Yee, M.J. Tobin, Molecular characterization of cyanobacterial silicification using synchrotron infrared micro-spectroscopy, Geochim. Cosmochim. Acta 68 (2004) 729–741.
[31] M. Dittrich, S. Sibler, Cell surface groups of two picocyanobacteria strains studied by zeta pontential investigations, potentionmetric titration, and infrared spectroscopy, J. Colloid Interface Sci. 286 (2005) 487–495.
[32] S.T. Akar, A. Gorgulu, Z. Kaynak, B. Anilan, T. Akar, Biosorption of reactive blue 49 dye under batch and continuous mode using a mixed biosorbent of macrofungus *Agaricus bisporus* and *Thuja orientails* cones, Chem. Eng. J. 148 (2009) 26–34.
[33] V. Erukhimovitch, V. Pavlov, M. Talyshinsky, Y. Souprun, M. Huleihel, FTIR microscopy as a method for identification of bacterial and fungal infections, J. Pharmaceut. Biomed. 37 (2005) 1105–1108.
[34] B.T. Low, Y.P. Ting, S.B. Deng, Surface modification of Penicillium chrysogenum mycelium for enhanced anionic dye removal, Chem. Eng. J. 141 (2008) 9–17.
[35] M.M. Dávila-Jiméneza, M.P. Elizalde-Gonzálezb, A.A. Peláez-Cid, Adsorption interaction between natural adsorbents and textile dyes in aqueous solution, Colloids Surf. A 254 (2005) 107–114.
[36] M.F. Hopgood, Nomogram for calculating percentage ionization of acids and bases, J. Chromatogr. A 47 (1970) 45–50.
[37] D.R. Lide (editor-in-chief), CRC Handbook of Chemistry and Physics, 90th ed., CRC Press, 2009–2010.
[38] P.P. Roy, S. Paul, I. Mitra, K. Roy, On two novel parameters for validation of predictive QSAR Models, Molecules 14 (2009) 1660–1701.
[39] V. Yangali-Quintanilla, A. Sadmani, M. McConville, M. Kennedy, G. Amy, A QSAR model for predicting rejection of emerging contaminants (pharmaceuticals, endocrine disruptors) by nanofiltration membranes, Water Res. 44 (2010) 373–384.
[40] A Naeem, J.R. Woertz, J.B. Feim, Experimental measurement of proton, Cd, Pb, Sr, and Zn adsorption onto the fungal species *Saccharomyces cerevisiae*, Environ. Sci. Technol. 40 (2006) 5724–5729.
[41] J.M. Tobin, D.G. Cooper, R.J. Neufeld, Uptake of metalions by Rhizopusarrhizus biomass, Appl. Environ. Microbiol. 47 (1984) 821–824.
[42] V.M. Nurchi, G. Crisponi, I. Villaescusa, Chemical equilibria in wastewaters during toxic metal ion removal by agricultural biomass, Coord. Chem. Rev. 254 (2010) 2181–2192.
[43] M. Franz, H.A. Arafat, N.G. Pinto, Effect of chemical surface heterogeneity on the adsorption mechanism of dissolved aromatics on activated carbon, Carbon 38 (2000) 1807–1819.
[44] C. Chen, J.L. Wang, Correlating metal ionic characteristics with biosorption capacity using QSAR model, Chemosphere 69 (2007) 1610–1616.
[45] S.S. Zamil, S. Ahmad, M.H. Choi, J.Y. Park, S.C. Yoon, Correlating metal ionic characteristics with biosorption capacity of *Staphylococcus saprophyticus* BMSZ711 using QICAR model, Bioresour. Technol. 100 (2009) 1895–1902.
[46] K.J. Kennedy, J.H. Lu, W.W. Mohn, Biosorption of chlorophenols to anaerobic granular sludge, Water Res. 26 (1992) 1085–1092.
[47] D.T. Stanton, P.C. Jurs, Development and use of charge partial surface area structural descriptors in computer-assisted quantitative structure–property relationship studies, Anal. Chem. 62 (1990) 2323–2329.
[48] S. Winiwarter, F. Ax, H. Lennernas, A. Hallberg, C. Pettersson, A. Karlen, Hydrogen bonding descriptor in the prediction of human in vivo intestinal permeability, J. Mol. Graph. Model. 21 (2003) 273–287.
[49] http://www.logP.com.